Eur. Polym. J. Vol. 29, No. 5, pp. 731–736, 1993
Printed in Great Britain.

0014-3057/93 $6.00 + 0.00

CO-PHOTOLYSIS OF POLYSTYRENE HYDROPEROXIDE WITH POLY(VINYLACETOPHENONE)

NEIL A. WEIR, J. ARCT and J. K. LEE
Chemistry Department, Lakehead University, Thunder Bay, Ontario, Canada P7B 5E1

(Received 1 June 1992)

Abstract—Films made from poly(styrene) hydroperoxide (PSOOH) and poly(vinylacetophenone) (PVAP) were exposed to long-wave ($\lambda \geqslant 300$ nm) u.v. radiation under high vacuum at $25 \pm 1°$. The presence of PVAP considerably enhanced the rate of decomposition of PSOOH, the quantum yield increasing by a factor of 2.5. New hydroxyl groups were formed as a result of photoreduction of the PVAP and of abstraction by the initially formed alkoxy radicals. In addition to the products of photolysis of PVAP (methane, ethane and CO), other low molecular weight species were detected, viz. water, CO_2, benzaldehyde, acetophenone, O_2 and benzene. The yield of CH_4 was about four times that produced from PVAP alone; this effect was attributed to abstraction of the hydroxylic H-atom of PSOOH by $CH_3^{\cdot}$ radicals from PVAP. Molecular weight and GPC measurements indicate that chain scission occurs in the earlier stages of the reaction, but its effects are rapidly overwhelmed by cross-linking, which appears to be particularly facile. The rate of decomposition of PSOOH is linearly dependent on the hydroperoxide content of the polymer and on the PVAP concentration at lower concentrations. However, higher PVAP concentrations lead to an accelerating rate of decomposition. The higher quantum yield for PSOOH disappearance is attributed to sensitized decomposition involving both $CH_3^{\cdot}$ radicals and keto groups from PVAP. The mechanism of these reactions are discussed.

INTRODUCTION

In addition to being decomposed by direct photolysis (i.e. O—O bond scission), both polymeric and low molecular weight hydroperoxides undergo sensitized decompositions following reactions with initially formed radicals, and with products of decomposition, like ketones [1–4]. Small, reactive free radicals, like hydroxyl, abstract the hydroxylic H-atom to form a peroxy radical, and triplet ($n \rightarrow \pi^*$) states of ketones act as photosensitizers, decomposing the hydroperoxide by energy transfer through the intermediary of an exciplex [2, 5, 6], and more importantly, by photoreduction, the hydroxylic H-atom again being abstracted [4].

While it is generally recognized that the hydroperoxide is a key intermediate in the photo and oxidative degradations of poly(styrene) (PS), it is not always appreciated that the initial decompositions (both thermal and photochemical) can provide the species which have been implicated in sensitized decompositions. Although a number of ketonic structures have been proposed, there is general agreement, based upon much experimental evidence, that an analogue of acetophenone, i.e. a terminal ketonic species, is the most abundant carbonyl product formed in the oxidative and photo-oxidative degradations of PS [8, 9]. It is derived from the β-scission of the initially formed polymeric alkoxy radical (PSO$^{\cdot}$), i.e.

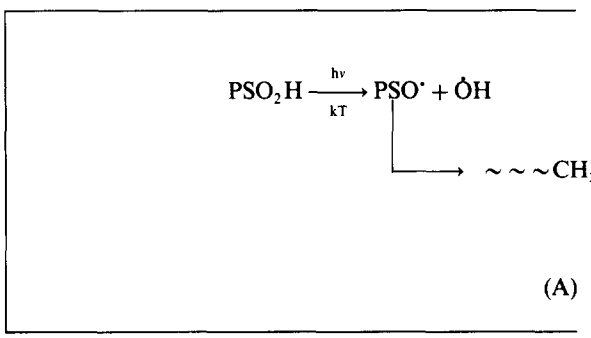

(1)

(A)

In a recent study of the photodecomposition of poly(styrene) hydroperoxide (PSOOH), it was observed that such sensitized decompositions accounted for the major part of the depletion of the hydroperoxide concentration, the direct photolysis contributing significantly only in the initial stages of the reaction [7].

The aim of the work now reported was to investigate the effect of a polymeric carbonyl compound on the long-wave ($\lambda \geqslant 300$ nm) photodecomposition of PSOOH; the polymer was chosen in preference to a low molecular weight ketone, on the grounds that this system bears a closer resemblance to the conditions which obtain during the actual photo-oxidative

degradation of PS [10]. Poly(vinylacetophenone) (PVAP) was chosen as the polymer for two reasons. Firstly, its photochemistry is well known [11, 12], and secondly, it is structurally similar to molecule (A) (above), and hence can be regarded as a plausible model compound for (A).

EXPERIMENTAL PROCEDURES

Materials

In order to avoid possible complications associated with polydisperse samples, PS was prepared by anionic polymerization at 0°, using a standard method with n-butyl lithium as catalyst [13]. Purification consisted of repeated precipitation of dichloromethane solutions in methanol, followed by drying and pumping at 10^{-6} torr (1 torr = 133.33 Pa). The molecular weight, $\bar{M}_n$ (membrane osmometry) was 8.7×10^4 and the polydispersity index was 1.16. This sample was used to prepare both the PSOOH and PVAP, the latter being formed by the acetylation of PS, using a procedure described elsewhere [14, 15]. PSOOH was prepared by the initiated oxidation of PS in dichloromethane at 35 ± 1°, the catalyst being di-t-butyl hyponitrite. Details of the method and of the purification are already published [7, 16]. The extent of hydroperoxidation was limited to *ca* 12% (base molar quantity) by controlling reaction times. Isolations of both PVAP and PSOOH were carried out using the same procedure as for PS, and the polymers were similarly dried and stored in the dark at 0°.

Photochemical techniques

Mixtures of PSOOH and PVAP were cast into films (5×10^{-2} mm thick) by solvent evaporation (CH_2Cl_2), pumped and stored under high vacuum in the dark. Concentrations of each component were independently varied, in order to test kinetic relationships. However, in order to maintain complete miscibility (as indicated by differential scanning calorimetry), the concentration of PVAP was limited to 16% (on a molar basis). Films were exposed to the output of a medium pressure Hg arc (200 W Hanovia), the incident radiation being restricted to wavelengths of $\geqslant 300$ nm, by means of a Pyrex (9–53 Corning) filter interposed between the source and the reaction vessel. The reaction temperature was maintained at 25 ± 1° by water circulation in the annular space of the double-walled reaction vessel. The presence of water also reduced the probability of additional thermal decomposition, by removing most of the i.r. radiation produced by the arc. More details of the equipment and experimental procedures are published elsewhere [12].

Quantum yields for some of the reactions were estimated using photochromic actinometry (Aberchrome 540) [17]. The fractions of light absorbed by solutions in the $300 < \lambda < 350$ nm range were estimated using an IL500 Research Radiometer in conjunction with a SEE 400 W photodiode (both International Light).

Analytical measurements

Reactions were investigated from three points of view, viz. PSOOH depletion, molecular weight changes and product formation. The hydroperoxide was determined quantitatively using a modified version of the method of Mitchell [18]. Number-average molecular weights were determined by membrane osmometry (Hewlett Packard 501) samples being irradiated for the requisite time, and dissolved immediately in toluene. Low molecular weight compounds ($m/e \leqslant 150$) were analysed on a continuous basis, using an in-line quadrupole mass spectrometer (Dataquad 200) [19]. Only water and methane were produced in sufficient quantity to justify quantitative analyses, and the equipment was calibrated using pure samples. Other spectroscopic techniques including FTIR (Brucker IFS66) and u.v. (Perkin–Elmer 1320) were used to monitor PSOOH decomposition and product formation, particularly in the ketone and hydroxyl regions of the i.r. spectrum.

RESULTS

Absorption of films in the long-wave region

The extents of absorption of mixtures of PSOOH and PVAP are small in the long-wave region ($\lambda \geqslant 300$ nm), being confined to a broad, structureless band ($300 < \lambda < 350$ nm) associated with the O—O chromophore, upon which is superimposed the symmetry forbidden $n \rightarrow \pi^*$ transition ($\lambda_{max} = 308$ nm) of the carbonyl. The corresponding molar absorption coefficients, ϵ_c (for PVAP) and ϵ_p (for PSOOH) are, respectively, 45 $dm^3\,mol^{-1}\,cm^{-1}$ and 0.6 $dm^3\,mol^{-1}\,cm^{-1}$ [7, 15], (measured arbitrarily at 310 nm); thus it can be seen that, even at low concentrations, PVAP is the principal absorber. It also follows that the total rate of absorption of quanta, I_a, given by the relation

$$I_a = I_0\{(1 - \exp[-\epsilon_c C_c/l]) + (1 - \exp[-\epsilon_p C_p l])\} \quad \text{(I)}$$

(I_0 is the incident intensity, l is the path length, and C is the concentration) can be approximated by:

$$I_a \approx I_0 l(\epsilon_c C_c + \epsilon_p C_p). \quad \text{(II)}$$

For the films, the products $\epsilon \times c$ can be replaced by absorption coefficients, β, so that according to Lambert's Law,

$$I_a \text{ becomes } I_0 l(\beta_c + \beta_p)(l = \text{film thickness}).$$

Values of β are difficult to measure with accuracy but values of 3 per cm and 200 per cm have been estimated for β_p and β_c, respectively [20]. In calculating the quantum yield for PSOOH decomposition, the rate of absorption of quanta over the range 300–350 nm was used, β_p being independent of wavelength (within experimental error) over this range.

Hydroperoxide decomposition

Data for the decomposition of PSOOH are shown in Fig. 1(A), in which the extent of decomposition is

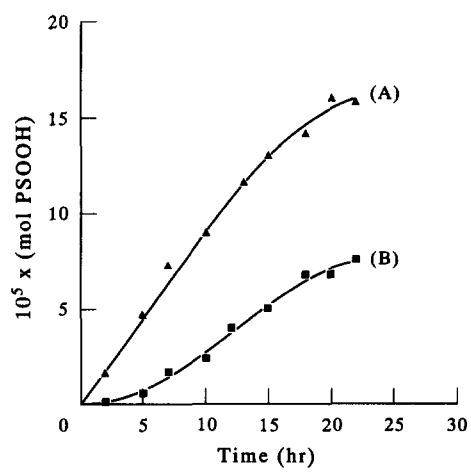

Fig. 1. Extent of decomposition of PSOOH (moles) as a function of time of irradiation under high vacuum ($\lambda \geqslant 300$ nm). (A) PSOOH + 6.8 mol% PVAP; (B) PSOOH only.

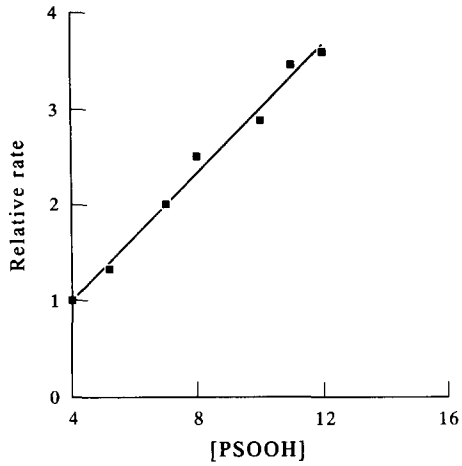

Fig. 2. Effect of hydroperoxide content (base molar quantity) on rate of decomposition of PSOOH during irradiation ($\lambda \geqslant 300$ nm) under high vacuum. Data shown as relative rates. (Rate = 1.00 for a hydroperoxide content of 4.0 b.m.u.)

shown as a function of the time of irradiation of a film containing both PSOOH and PVAP. Similar data are shown [Fig. 1(B)] for a film containing PSOOH only; it can be seen that the presence of PVAP not only increases the rate of degradation but also alters its characteristics.

The quantum yield for PSOOH decomposition (PVAP present) was 4.8 ± 0.5 mol (einstein)$^{-1}$ and it was found to be dependent on the hydroperoxide content; thus, the above value [hydroperoxide content 6.5% (base molar quantity)] increased to 6.1 ± 0.6 mol einstein)$^{-1}$ when the hydroperoxide concentration was 12% (base molar quantity).

The effect of hydroperoxide content on the rate was investigated; the results are shown in Fig. 2 where the relative rate is shown as a function of hydroperoxide content [rate = 1.00 for a hydroperoxide content of 4% (base molar quantity)]. In all cases the PVAP concentration was 5 mol%. While there is a good correlation between the two variables at higher hydroperoxide concentrations, >4%, the linearity is not maintained as the concentration decreases; this effect is probably attributable to analytical uncertainties rather than to some direct kinetic effect.

Data showing the relationship between rate and the PVAP concentration are shown in Fig. 3, in which the relative rate is plotted as a function of PVAP concentraiton (in mol%) (rate = 1.00 when the PVAP concentration is 2 mol%). It can be seen that, except for the highest concentrations, there is a reasonable correlation between the two quantities, and such behaviour can be reconciled with the form of equation (II).

Spectroscopic changes

Changes were observed in the hydroxyl (3400–3650 cm^{-1}) and in the carbonyl (1680–1750 cm^{-1}) regions. In the former case, the intensity of the peak at 3440 cm^{-1} (due to the hydroperoxide) decreased, and there was a simultaneous, general increase in absorption over the 3540–3650 cm^{-1} range. However, definite maxima could be distinguished at 3465 and 3550 cm^{-1}. Changes in the carbonyl region were smaller, being restricted to a broadening of the 1685 cm^{-1} absorption, and to a concomitant increase in absorption in the 1725–1750 cm^{-1} region.

Low molecular weight products

M.s. analyses indicated the formation of a complex mixture of volatile products having $m/e < 150$. The most abundant were methane and water but smaller amounts of CO_2, CO, ethane and acetophenone, and traces of benzaldehyde and benzene were also detected. Characteristics of formation of CH_4 and H_2O are shown in Fig. 4 (A and B), from which it can be seen that, after an initial, essentially constant rate of evolution, the rates of formation decline on longer exposures. Quantum yields for H_2O and CH_4 formation were estimated to be 5×10^{-2} and 5×10^{-3} ($\pm 10\%$) mol(einstein)$^{-1}$ respectively, both values being greater than those obtained from the photolyses of either polymer on its own [7, 15].

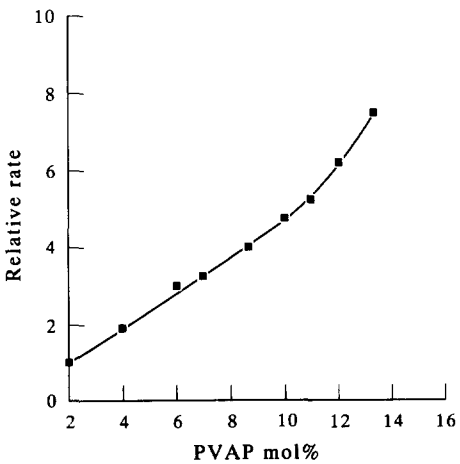

Fig. 3. Effect of PVAP concentration on the decomposition of PSOOH during irradiation ($\lambda \geqslant 300$ nm) under high vacuum. Rate = 1.00 when the PVAP concentration is 2 mol%.

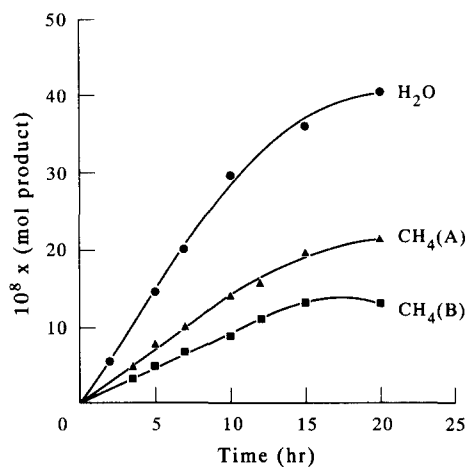

Fig. 4. Low molecular weight products from the photolysis of PSOOH ($\lambda \geqslant 300$ nm) under high vacuum. (A) In presence of PVAP; (B) in presence of PS.

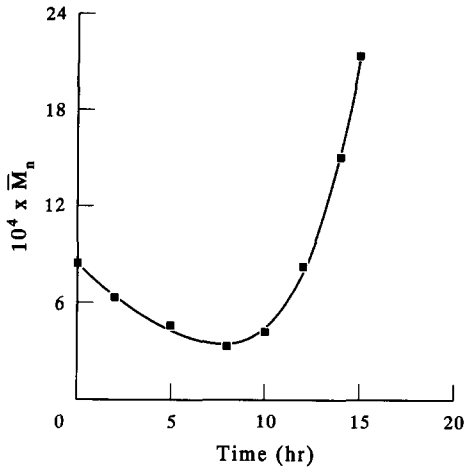

Fig. 5. Molecular weight ($\bar{M}_n$) changes as a function of time of irradiation ($\lambda \geqslant 300$ nm) under high vacuum of PSOOH containing 8 mol% PVAP.

In order to estimate the extent of the methyl radical reaction (abstraction) with the hydroxylic H-atom of PSOOH, the irradiation was repeated under identical conditions, PSOOH being replaced by PS. The data in Fig. 4(C) clearly indicates that the methane yield is increased when PSOOH is present. The yield of ethane is also increased when PS is present, reflecting the lower probability of the methyl radicals in abstraction reactions with PS.

Molecular weight changes

Changes occur in both the number-average molecular weight and in the polydispersity index. Typical data are shown in Fig. 5; after an initial decrease, the molecular weight increases very rapidly, indicating that cross-linking occurs to a greater extent as the decomposition proceeds. The molecular weight distribution rapidly broadens and becomes skewed towards higher molecular weights. It was difficult to investigate the polydispersities, on account of the adverse effects of highly cross-linked polymers on the GPC columns.

It is appreciated that PVAP itself undergoes molecular weight changes upon irradiation. However, the error introduced into the molecular weight data by the presence of 6.5 mol% of PVAP is unlikely to be significantly greater than the intrinsic experimental errors.

DISCUSSION

It has been established [11] that upon long-wave ($\lambda \geqslant 300$ nm) irradiation, PVAP undergoes a Norrish Type I photodecomposition, CH_3—C=O bond fission being favoured, and that the triplet $n \rightarrow \pi^*$ carbonyl also undergoes photoreduction, the tertiary H-atom in the chain being abstracted.

i.e.

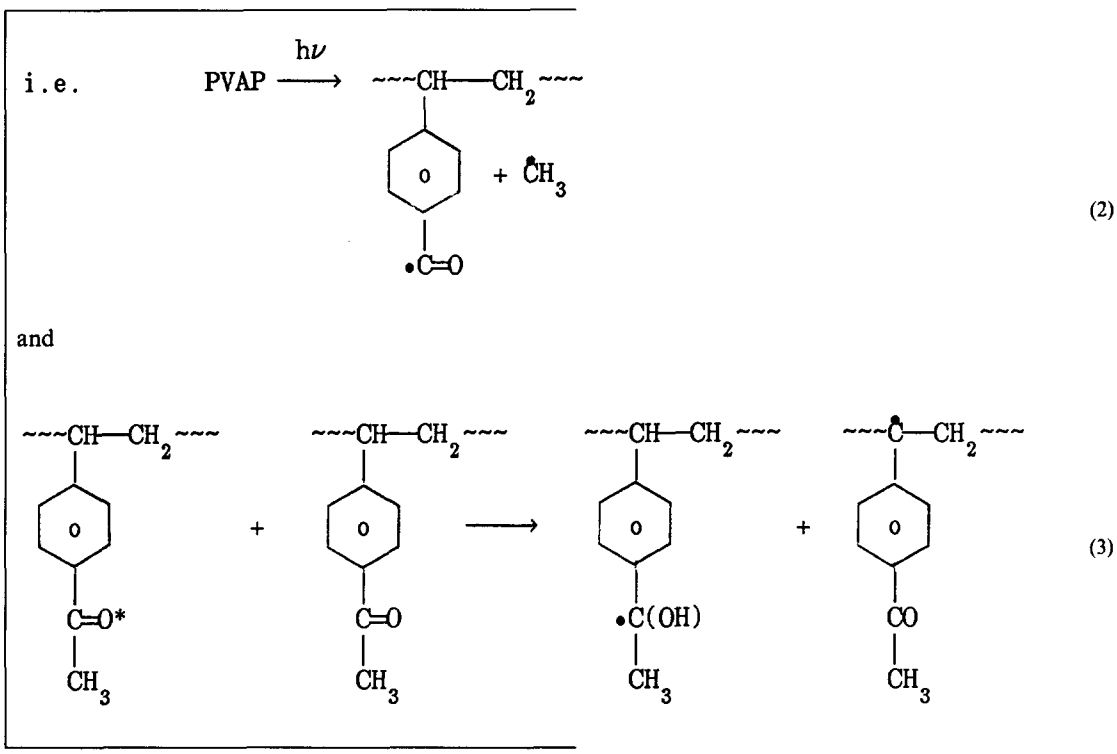

In the presence of PS, the results are qualitatively similar; however, PS also participates in photoreduction reactions and methane is formed by methyl radical abstraction of the tertiary H-atoms in PS [15].

Absorption of long-wave quanta by polymeric hydroperoxides leads to their dissociation (O—O bond scission), quantum yields in many cases exceeding unity [2–4], the value frequently associated with the photolysis of low molecular weight compounds [21].

PSOOH also absorbs in this spectral region, the initial decomposition being represented by equation (1) [5, 10]. More recently, however, it has been shown that the overall decomposition of PSOOH cannot be represented by equation (1) alone, and that the predominant modes of decomposition involve reactions of PSOOH with initially formed radicals and carbonyl compound, formed as in equation (1) [7].

It is clear from the present results that PVAP influences the rate and the characteristics of the degradation of PSOOH. In particular, the rate of decomposition depends on the PVAP concentration (Fig. 3); the quantum yield is considerably greater than that obtained from the photolysis of PSOOH alone [i.e. 2 ± 0.25 mol(einstein)$^{-1}$]; the extent of cross-linking in the polymer blend is greater, as are the range and abundances of products. To account for these and other observations, the following additional decomposition mechanisms are considered.

(a) Reactions with radicals

Previous work indicates that the OH (and perhaps also the PSO) radical interacts with the hydroxylic H-atom [7]. The results shown in Fig. 4, together with the larger value of the quantum yield for CH_4 formation, are explicable in terms of additional decomposition of PSOOH, induced by reaction with the methyl radical, i.e.

$$^{\cdot}CH_3 + PSOOH \rightarrow CH_4 + PSO_2^{\cdot} \quad (4)$$

The higher CH_4 yield from the blend (*cf.* PS) is attributable to the preferential abstraction of the hydroxyl H-atom, bond energy-bond order calculations, indicating that the O—H is considerably more reactive than the C—H, in spite of their having comparable bond dissociation energies [22]. This result is of some relevance to the photo-oxidation of PS, since methyl radicals could be produced by the photolysis of some of the methyl ketone products which have been proposed [9].

The resulting tertiary peroxy radicals combine to form a tetroxide, which subsequently decomposes to form a peroxide, alkoxy radicals and O_2 [23], i.e.

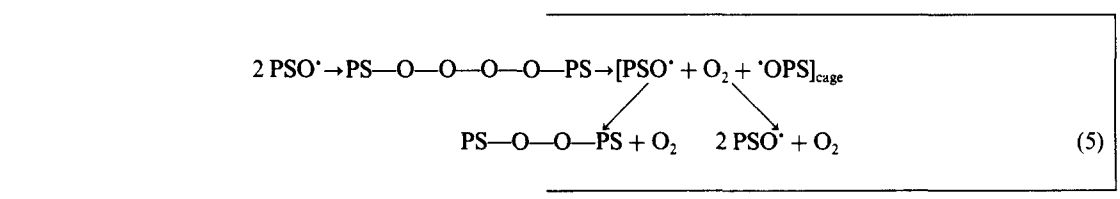

Such a reaction would account for the production of O_2, and the appearance of a new i.r. absorption around 3550 cm^{-1} is consistent with the formation of hydroxylic species, alkoxy radicals readily undergoing abstraction reactions.

Recent studies [24] indicate that tertiary peroxy radicals combine [as in equation (5)] in preference to undergoing abstraction; thus the regeneration of PSOOH by abstraction, though not impossible, would not be expected to compete significantly with the degradation.

(b) Reaction with carbonyls

The enhanced rate of degradation of PSOOH (Fig. 1) together with the high quantum yield for its disappearance cannot be reconciled with (a) above alone. Other studies have shown that carbonyl triplets play a major role [2–4], thus the results can be better understood in terms of additional sensitized decomposition. Two distinct processes are involved. In the former case, decomposition results from a vibrationally excited hydroperoxide, an exciplex, in which electronic energy from the triplet is transferred to the vibrational manifold of the hydroperoxide being involved, i.e.

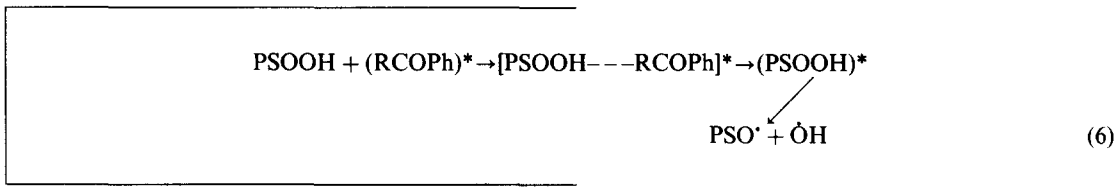

The net effect of equation (6) is to increase the quantum yield for H_2O formation and the yields of hydroxylic compounds Geuskens has shown that [equation (6)] plays an important part in the photo-oxidation of PS [6].

An alternative quenching mechanism, which has been shown to lead to most of the hydroperoxide decomposition, is that in which the carbonyl triplet is photoreduced, the hydroxylic H-atoms of the hydroperoxide being abstracted [6], i.e.

$$(RCOPh)^* + PSOOH \rightarrow R\dot{C}(OH)Ph + PSO_2^{\cdot} \quad (7)$$

(B)

This reaction not only provides an additional source of peroxy radicals, but also a precursor (B) for a pinacol (formed by abstraction) which has been associated with the i.r. absorption at 3465 cm^{-1} [15].

Carbonyl products arising from PSOOH decomposition can also contribute to the sensitized decompositions [1], and this point is reflected in the value of the quantum yield for PSOOH disappearance.

These results, which have an important bearing on the photo-oxidation of PS, demonstrate conclusively that macro-ketones play an important part in the

overall degradation process, by sensitizing hydroperoxide decomposition.

Some of the low molecular weight volatiles can be accounted for in terms of the photolysis of carbonyls, like (A) (Norrish Types I and II photodecompositions), i.e.

Type I

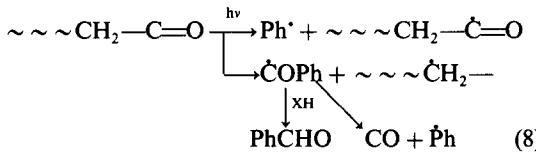

(8)

$$Ph^{\cdot} + XH \rightarrow C_6H_6 + X^{\cdot} \quad (9)$$

(XH contains an abstractable H-atom).

Type II

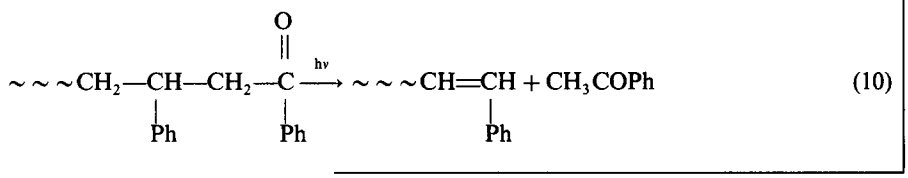

(10)

Quantum yields are, however, very low [$< 10^{-5}$ mol (einstein)$^{-1}$].

Molecular weight changes

The data in Fig. 5, together with the observed increasing polydispersities, indicate that simultaneous chain scission and cross-linking occur. Chain scission can be attributed to β-scission in the alkoxy (PSO) radical [(as in equation (1)]. However, it is not only less probably than abstraction (typical rate constants being of the order of $10^4\,sec^{-1}$ and $10^6\,M^{-1}\,sec^{-1}$ for scission and abstraction, respectively) [3] but it is also subject to inhibition, the separation of macrofragments being impeded by the higher microviscosity of the solid state. In addition, the effects of chain scission are diminished by competing cross-linking, which in turn can be brought about by interactions not only of primary (e.g. PSO$^{\cdot}$ and PSO$_2^{\cdot}$) but also of secondary radicals, the latter being formed at the tertiary C-atoms in the chains, as a result of abstraction with, for example, ȮH radicals.

The apparent reduction in rate of product evolution (Fig. 4) can be attributed to cross-linking, which leads not only to a reduction in the diffusion coefficients for the gaseous products [25] but also reduces the flexibility of the system and renders the approach of the triplet carbonyl to the hydroperoxy group more difficult. Consequently the specific geometric orientations required for optimal interaction (critical for energy transfer), cannot always be achieved.

Acknowledgement—The authors gratefully acknowledge the financial support of the Natural Sciences and Engineering Research Council of Canada.

REFERENCES

1. R. Hiatt, J. Clipshom and T. Visser. *Can. J. Chem.* **42,** 2754 (1964).
2. H. C. Ng and J. E. Guillet. *Macromolecules* **11,** 937 (1978).
3. S. K. L. Li and J. E. Guillet. *ibid.* **17,** 41 (1984).
4. L. C. Stewart, D. J. Carlsson, D. M. Wiles and J. C. Scaiano. *J. Am. chem. Soc.* **105,** 3605 (1983).
5. G. Geuskens, D. Baeyens-Volant, D. Delaunois, Q. Lu Vinh, W. Piret and C. David. *Eur. Polym. J.* **14,** 299 (1978).
6. G. Geuskens and C. David. *Pure Appl. Chem.* **51,** 233 (1979).
7. A. Ceccarelli and N. W. Weir. *Polym. Degrad. Stab.* (in press).
8. G. A. George and D. K. C. Hodgeman. *Eur. Polym. J.* **13,** 63 (1977).
9. J. Lucki and B. Rånby. *Polym. Degrad. Stab.* **1,** 165 (1979).
10. N. A. Weir. In *Developments in Degradation*, Vol. 4 (edited by N. Grassie). Applied Science Elsevier, London (1982).
11. N. A. Weir and T. H. Milkie. *J. Polym. Sci.; Polym. Chem. Edn* **17,** 3723 (1979).
12. N. A. Weir and K. Whiting. *Eur. Polym. J.* **26,** 991 (1990).
13. L. J. Fetters. *J. Res. Natn. Bur. Stand.* **70A,** 421 (1966).
14. D. Braun, W. Kern and H. Cherdron. *Techniques of Polymer Synthesis and Characterization*. Wiley, New York (1971).
15. N. A. Weir, M. Rujimethabas and P. Q. Clothier. *Eur. Polym. J.* **17,** 431 (1981).
16. H. Kiefer and T. G. Traylor. *Tetrahedron Lett.* 6163 (1966).
17. H. G. Heller and J. R. Langdon. *J. Chem. Soc., Perkin II,* 341 (1968).
18. J. Mitchell and L. R. Perkins. *Appl. Polym. Symp.* **4,** 167 (1967).
19. N. A. Weir and T. H. Milkie. *Polym. Degrad. Stab.* **1,** 105 (1979).
20. A. Ceccarelli and N. A. Weir. Unpublished data.
21. M. Nowakowska. In *Advances in the Stabilization and Controlled Degradation of Polymers*, Vol. 1 (edited by A. V. Patsis). Technomic Publishing, Basel (1989).
22. C. M. Previtali and J. C. Scaiano. *J. Chem. Soc., Perkin Trans.* **2,** 934 (1975).
23. J. A. Howard. In *Free Radicals*, Vol. II (edited by J. Kochi). Wiley, New York (1977).
24. L. A. Travadyan, M. V. Musaelyn and V. A. Mardoyan. *Khim. Fiz.* **10,** 511 (1991).
25. R. Greenwood and N. A. Weir. *J. appl. Polym. Sci.* **19,** 1409 (1975).